Electronic supplementary information

The selective oxidation of thioanisole to sulfoxide using a highly efficient electroenzymatic cascade system

Xuefang Zhu,[a] *Xiyue Liu,*[a] *Yu Ding,*[b] *Shuni Li,*[a] *Yucheng Jiang,**, [a] *and Yu Chen**, [b]

[a] Key Laboratory of Macromolecular Science of Shaanxi Province, School of Chemistry & Chemical Engineering, Shaanxi Normal University, Xi'an 710119, China.

[b] School of Materials Science and Engineering, Shaanxi Normal University, Xi'an 710119, China.

Corresponding authors:

E-mail: jyc@snnu.edu.cn (Y. Jiang)

E-mail: ndchenyu@gmail.com (Y. Chen)

Experimental section

Physical characterization

The crystal structure and composition of the samples were analyzed by powder X-ray diffraction (PXRD) patterns (DX-2700 power X-ray diffractometer) and X-ray photoelectron spectroscopy (XPS) (AXIS ULTRA spectrometer), respectively. The morphology of the samples was characterized by scanning electron microscopy (SEM, SU8220) and transmission electron microscopy (TEM, Tecnai G2 F20). Confocal laser microscopy (CLSM) images were acquired by In Via Reflex (Renishaw Co., Ltd, UK). The UV-vis spectra were recorded using UV-vis spectroscopy (Cary 60). The zeta (ζ) potentials were carried out by Malvern Zetasizer Nano ZS90. NMR spectra were obtained with Bruker Avance-III 600 NMR spectrometers at ambient temperature. Mass spectrum measurements were recorded on a Bruker high-resolution liquid mass spectrometer (Maxis Ultimate 300hplc). The crystal structure of CPO was obtained from a protein data bank (PDB ID: 1CPO) for molecular docking. Open Babel GUI software was used to prepare the input files. The docking results were visualized and analyzed with Discovery Studio 4.1 Visualizer.

The calculation of the CPO-IL_{EMB} loading amounts

The formula for calculating the loading amounts of CPO-IL_{EMB} is as follows:[1]

$$\text{loading amounts (mg g}^{-1}) = \frac{\Delta A \times V \times 42000}{\varepsilon \times l \times m} \quad (1)$$

Where ΔA is the value of absorbance change of CPO-IL_{EMB} at 398 nm; V denotes the final volume of the experiment (mL); ε is the molar absorbance coefficient of CPO (91200 L mol^{-1} cm^{-1});[2] l is the width

Electrochemical tests

Electrochemical experiments were carried out using a CHI 760E workstation (ChenHua, China) with a three-electrode system consisting of a working electrode, a carbon rod electrode as a counter electrode, and a saturated calomel electrode (SCE) as a reference electrode. All

electrochemical measurements were carried out in an H-cell separated by a proton exchange membrane (Nafion 117).

Determination of H_2O_2 through UV-vis method

An H-type cell was used to detect the Faraday efficiency and yield of H_2O_2 at NMCNs-PEI and CPO-IL_{EMB}@NMCNs-PEI biohybrid. First, the NMCNs-PEI and CPO-IL_{EMB}@NMCNs-PEI biohybrid were electrolyzed in 40 mL N_2-saturated 0.1 mol L^{-1} PBS (pH 5.0) for 30 min to subtract background. Then, the NMCNs-PEI and CPO-IL_{EMB}@NMCNs-PEI biohybrid were performed in O_2-saturated 0.1 mol L^{-1} PBS (pH 5.0) for 1 h at different potentials (from -0.3 V to -0.5 V *vs.* SCE).[3]

$$2Ce^{4+} + H_2O_2 \rightarrow 2H^+ + 2Ce^{3+} + O_2 \quad (2)$$

The UV-vis characteristic absorbance for Ce^{4+} was at 318 nm. Therefore, by determining the concentration of Ce^{4+}, the concentration of H_2O_2 can be calculated.

Determination of reactants and products through HPLC method

The products and reactants were determined by high performance liquid chromatography (HPLC) on a chiral column (5 μm, 4. 6 mm × 250 mm, Chiralpak) with the mobile phase of n-hexane: isopropyl (80:20). The detection wavelength, column temperature and flow rate were 254 nm, 28°C and 0.6 mL min^{-1}, respectively. The chiral separation of the oxidation product of thioether was performed using the chiral column (5 μm, 4.6 mm × 250 mm, Chiralpak). The mobile phase was constituted by n-hexane: ethanol at 80:20. Moreover, the column temperature is 14°C, and flow rate is set at 0.4 mL min^{-1}, and detection wavelength at 254 nm.

Figures

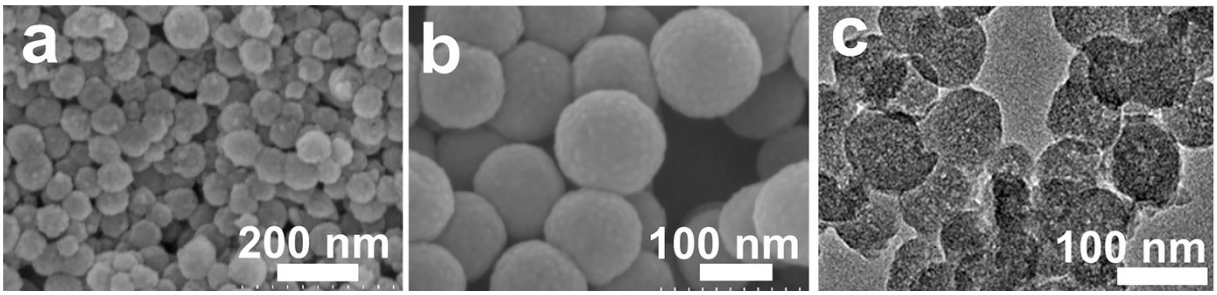

Fig. S1 (a, b) SEM images, and (c) TEM image of TMB/F127/PDA polymer.

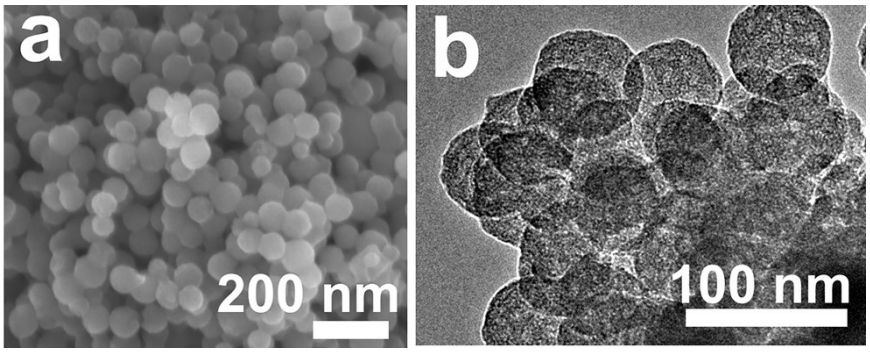

Fig. S2 (a) SEM image and (b) TEM image of NMCNs.

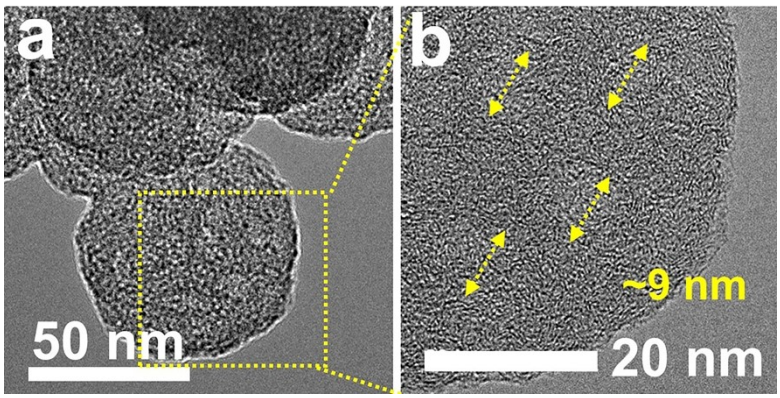

Fig. S3 (a) TEM image, and (b) HR-TEM image of NMCNs-PEI.

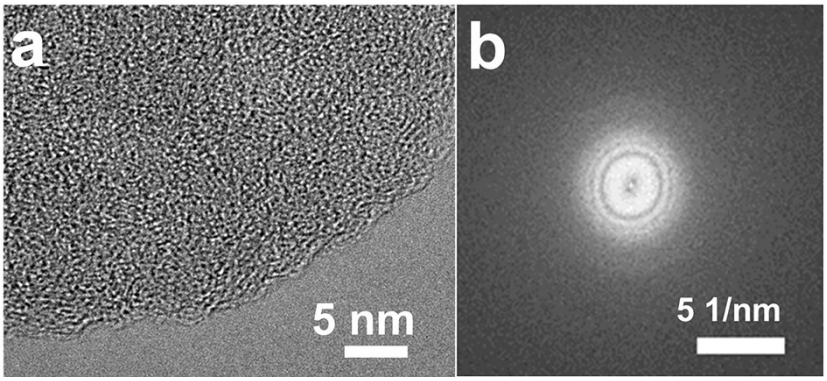

Fig. S4 (a) HR-TEM image and (b) the fractional Fourier transform of NMCNs-PEI.

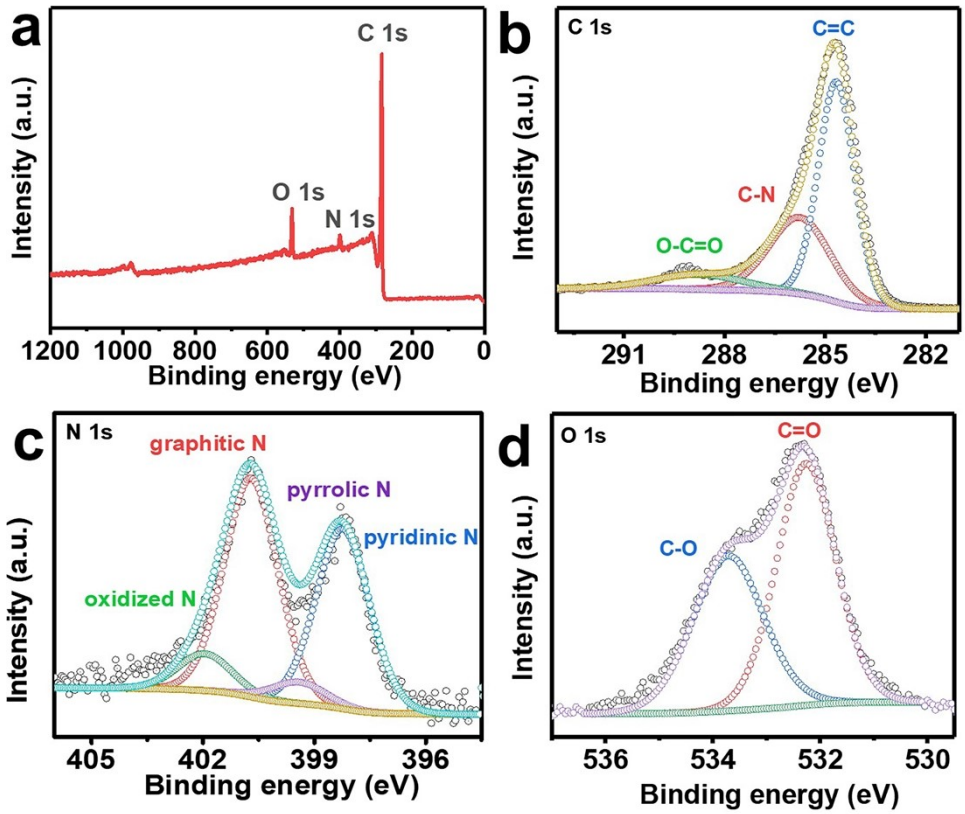

Fig. S5 (a) The full XPS spectrum, (b) C 1s XPS spectrum (c) N 1s XPS spectrum, and (d) O 1s XPS spectrum of NMCNs-PEI. In the high-resolution C 1s XPS spectrum, the C=C, C-N, and O-C=O functional groups can be observed at 284.6 eV, 285.9 eV, and 288.9 eV (Fig. S5b). Deconvoluting the N 1s XPS spectrum displays four peaks at 398.4, 399.5, 400.7, and 402.4 eV, which correspond to pyridinic N, pyrrolic N, graphitic N, and oxidized N, respectively (Fig. S5c). The O 1s XPS spectrum reveals two peaks at 532.3 and 533.7 eV, which correspond to C=O and C-O, respectively (Fig. S5d).

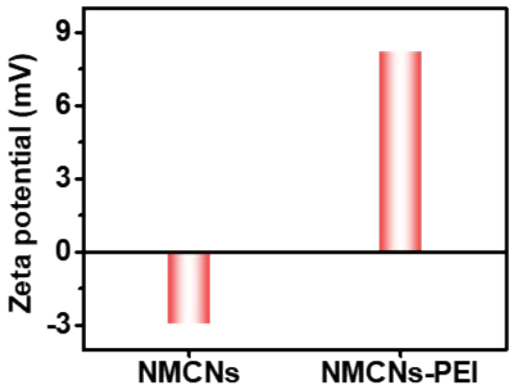

Fig. S6 The zeta potential of NMCNs and NMCNs-PEI.

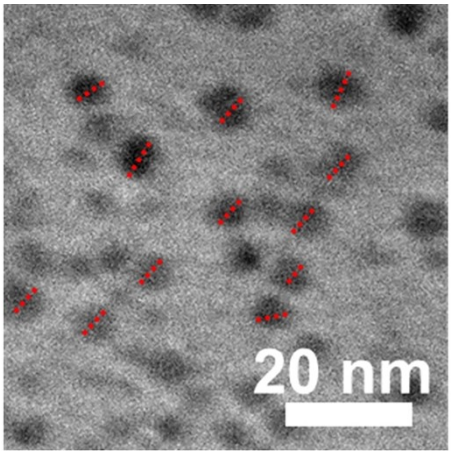

Fig. S7 TEM images of CPO.

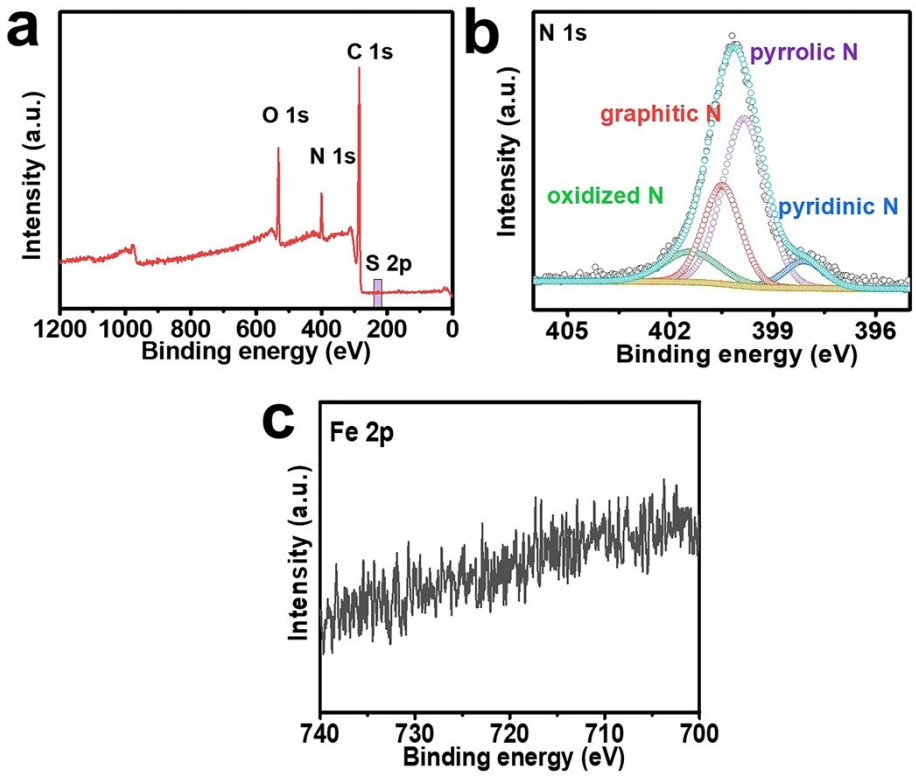

Fig. S8 (a) The XPS full spectrum, (b) N 1s XPS spectrum, and (c) Fe 2p XPS spectrum of CPO-IL_{EMB}@NMCNs-PEI biohybrid.

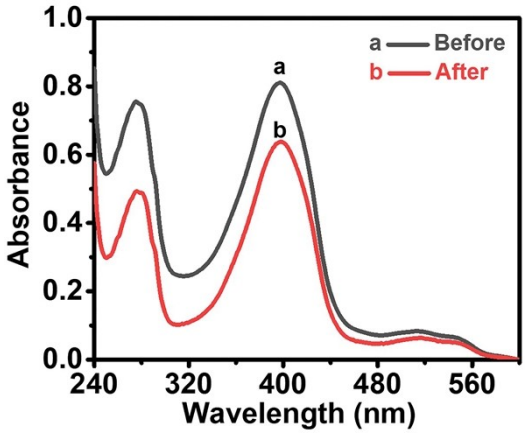

Fig. S9 The UV-vis spectra of the CPO-IL_{EMB} supernatant before and after loading on NMCNs-PEI.

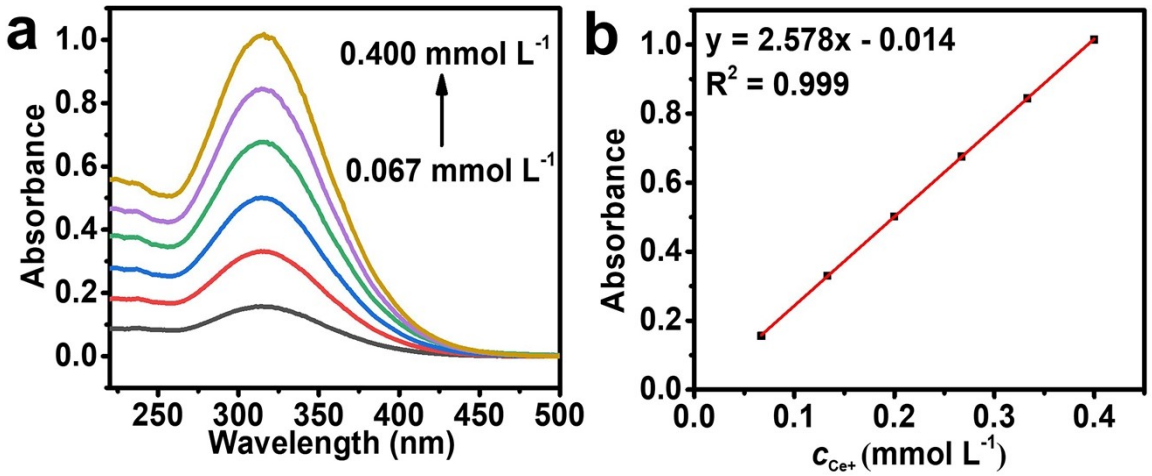

Fig. S10 (a) UV-vis curves of various Ce^{4+} concentrations, and (b) the standard curve of Ce^{4+} at the range of concentration from 0.067 mmol L^{-1} to 0.400 mmol L^{-1}).

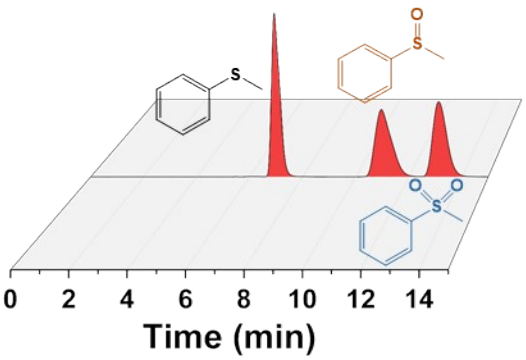

Fig. S11 The HPLC plots of standard samples of thioanisole, methyl phenyl sulfoxide, methyl phenyl sulfone. The retention times of thioanisole, methyl phenyl sulfoxide and methyl phenyl sulfone are 6.5 min, 10.9 min, and 13.0 min, respectively. The corresponding standard curves show good linear relationships with a correlation coefficient of 0.999 (see ESI, Fig. S11, S12, S13, and S14†).

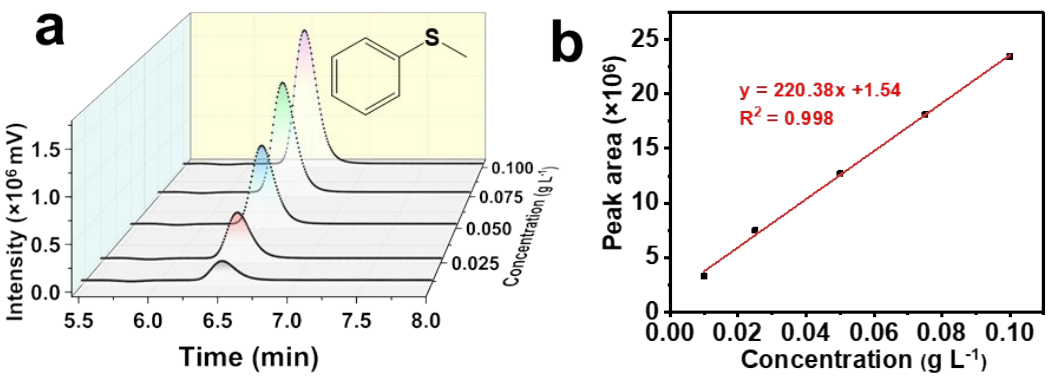

Fig. S12 (a) HPLC chromatograms and (b) the standard curve of thioanisole at the range of concentration from 0.01 to 0.1 g L^{-1}.

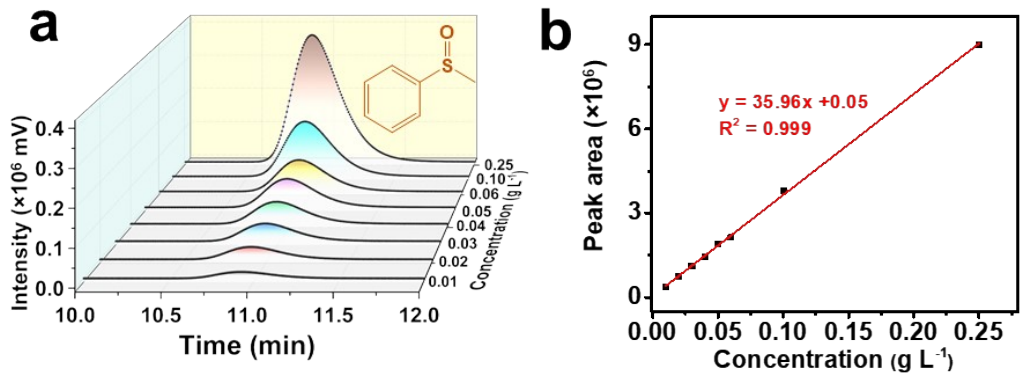

Fig. S13 (a) HPLC chromatograms and (b) the standard curve of methyl phenyl sulfoxide at the range of concentration from 0.01 to 0.25 g L^{-1}.

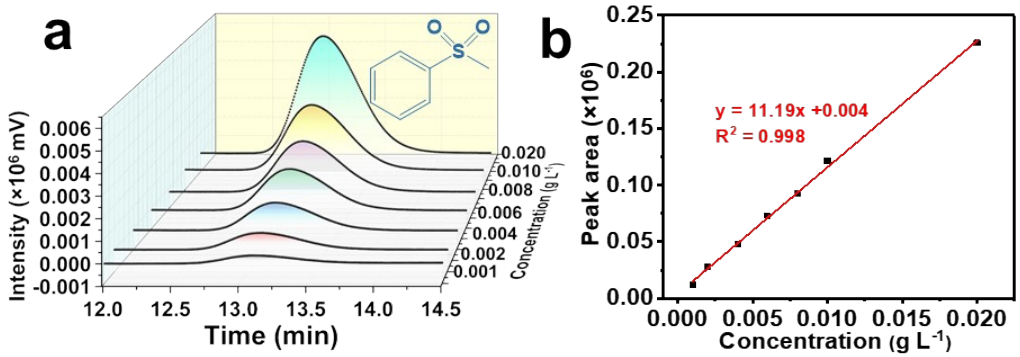

Fig. S14 (a) HPLC chromatograms and (b) the standard curve of methyl phenyl sulfone at the range of concentration from 0.001 to 0.02 g L^{-1}.

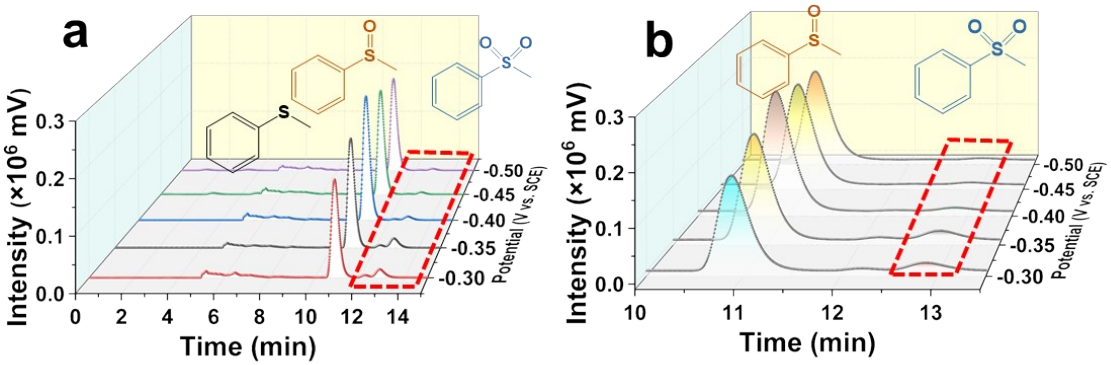

Fig. S15 (a) HPLC chromatograms of the product of oxidation of thioanisole by CPO-IL_{EMB}@NMCNs-PEI biohybrid in O_2-saturated PBS at different potentials, and (b) enlarged plot of retention time from 10 min to 13.5 min.

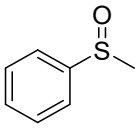

^{1}H NMR (600 MHz, $CDCl_3$) δ 7.31 – 7.26 (m, 4H), 7.14 (m, 1H), 2.49 (s, 3H).

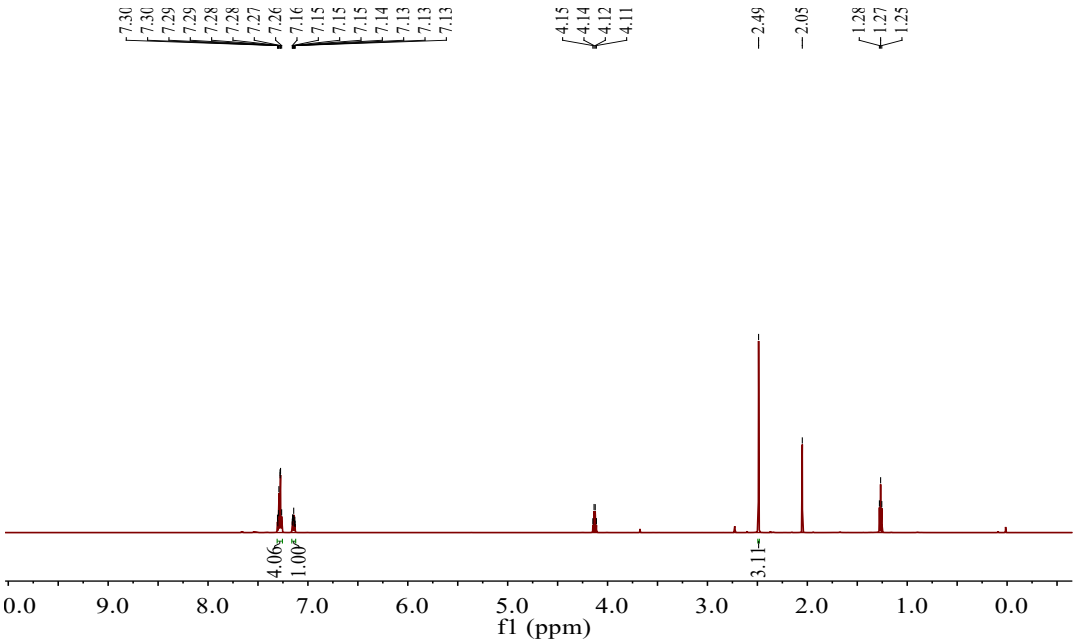

Fig. S16 ^{1}H NMR spectrum of oxidation product of thioanisole catalyzed by CPO-IL_{EMB}@NMCNs-PEI biohybrid at –0.4 V vs. SCE.

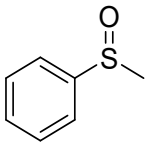

^{13}C NMR (151 MHz, $CDCl_3$) δ 138.5, 128.9, 126.7, 125.1, 60.5.

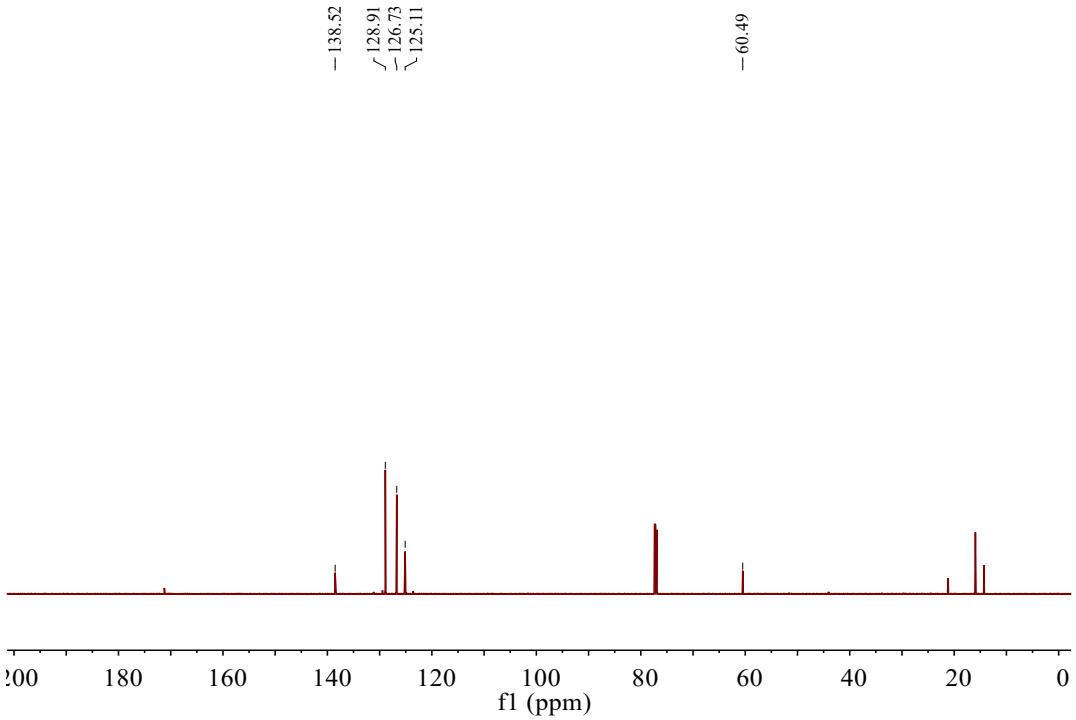

Fig. S17 ^{13}C NMR spectrum of oxidation product of thioanisole catalyzed by CPO-IL_{EMB}@NMCNs-PEI biohybrid at –0.4 V vs. SCE.

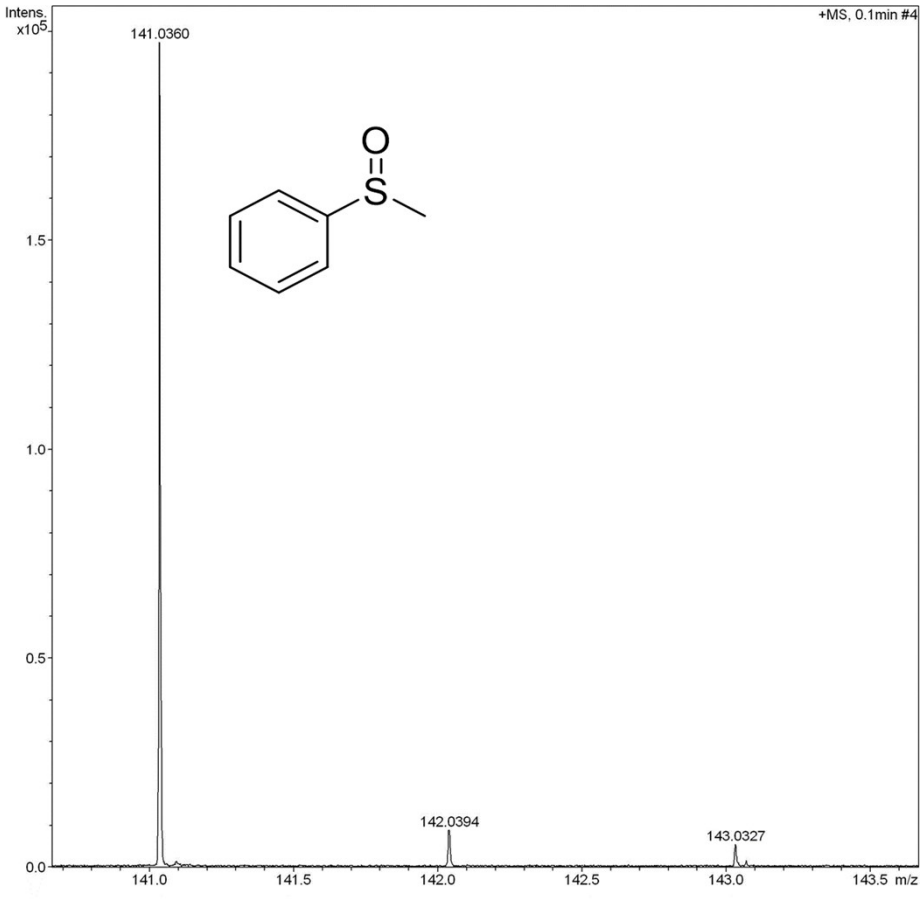

Fig. S18 Mass spectrum of oxidation product of thioanisole catalyzed by CPO-IL_{EMB}@NMCNs-PEI biohybrid at –0.4 V vs. SCE.

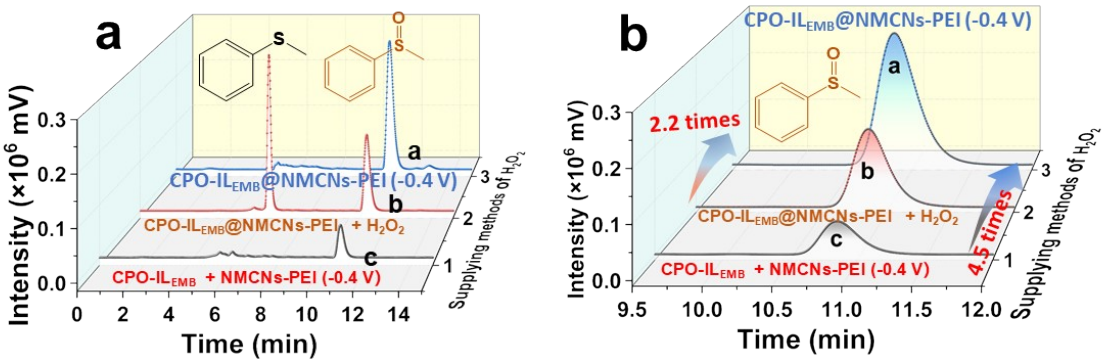

Fig. S19 (a) at –0.4 V for 1 h by CPO-IL_{EMB}@NMCNs-PEI biohybrid (curve a), CPO-IL_{EMB}@NMCNs-PEI biohybrid with adding H_2O_2 (curve b), and free CPO-IL_{EMB} by NMCNs-PEI biohybrid at –0.4 V for 1 h (curve c) and (b) enlarged plot of retention time from 9.5 min to 12 min.

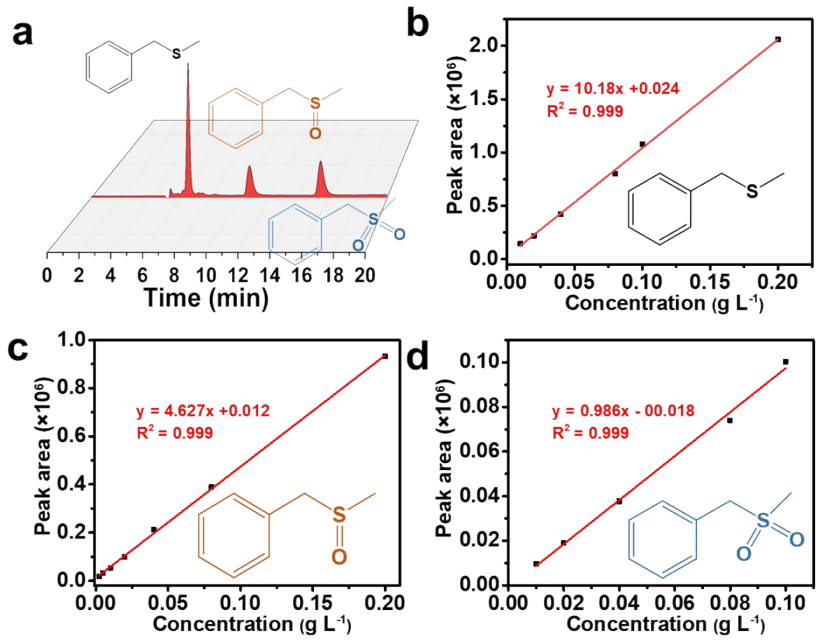

Fig. S20 (a) HPLC chromatograms of benzyl methyl sulfide, benzyl methyl sulfoxide and benzyl methyl sulfone, and the standard curves of (b) benzyl methyl sulfide, (c) benzyl methyl sulfoxide and (d) benzyl methyl sulfone. The retention times of benzyl methyl sulfide, benzyl methyl sulfoxide and benzyl methyl sulfone are 6.5 min, 10.7 min, and 15.5 min, respectively. The corresponding standard curves show good linear relationships with a correlation coefficient of 0.999 (see ESI, Fig. S20†).

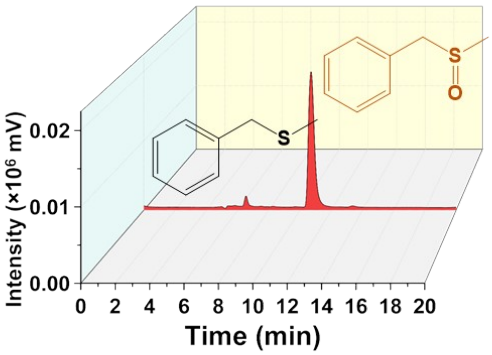

Fig. S21 HPLC chromatograms of oxidized product of benzyl methyl sulfide by CPO-IL_{EMB}@NMCNs-PEI biohybrid in O_2-saturated PBS at –0.4 V vs. SCE.

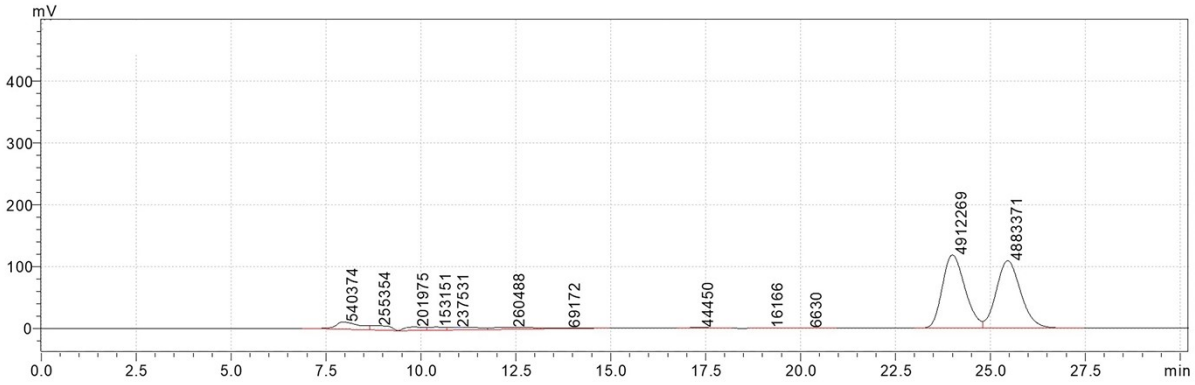

Fig. S22 HPLC chromatograms of oxidized product of thioanisole.

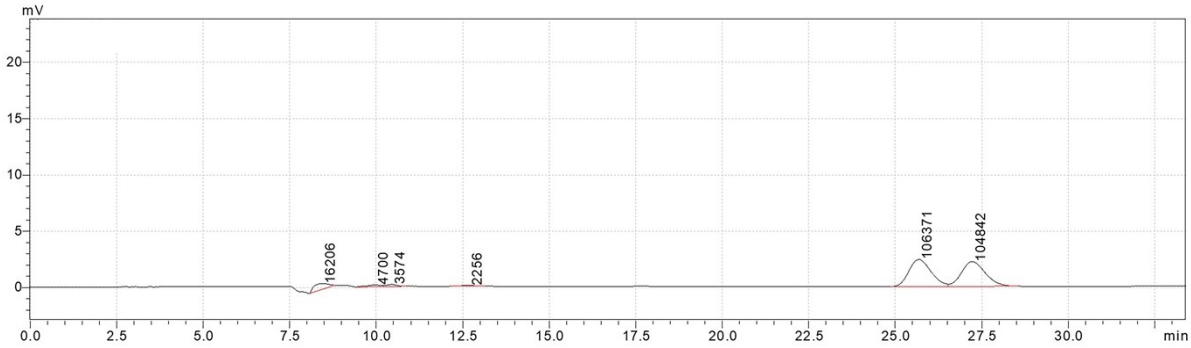

Fig. S23 HPLC chromatograms of oxidized product of benzyl methyl sulfide.

Table S1 Binding energy scores of molecular docking: CPO with thioanisole.

Mode	**Affinity**	**Dist from the best mode**	
		rmsd l.b.	rmsd u.b.
1	–4.8	0.000	0.000
2	–4.6	1.389	1.837
3	–4.5	1.924	3.810
4	– 4.2	4.102	5.308
5	–4.1	4.125	5.059
6	–4.1	3.478	4.617
7	–4.0	3.406	4.639
8	– 4.0	4.234	5.458
9	–3.7	5.117	6.552

Reference

1 X. Zhu, X. Fan, H. Lin, S. Li, Q. Zhai, Y. Jiang and Y. Chen, *Adv. Energy Mater.*, 2023, **13**, 2300669.

2 J. Lu, L. Cheng, Y. Wang, Y. Ding, M. Hu, S. Li, Q. Zhai and Y. Jiang, *Mater. Des.*, 2017, **129**, 219–226.

3 J. Zhu, X. Xiao, K. Zheng, F. Li, G. Ma, H. C. Yao, X. Wang and Y. Chen, *Carbon N. Y.*, 2019, **153**, 6–11.